

An Experimental Investigation of a Jet Issuing from a Wing in Crossflow

W. Mikolowsky* and H. McMahon†
Georgia Institute of Technology, Atlanta, Ga.

The aerodynamic interference resulting from a jet issuing normal to the chordal plane of a two-dimensional wing in a crossflow has been experimentally investigated. Measurements of the interference surface pressure distribution on the wing and of the wing interference force and moment coefficients have been made for a systematic variation of jet exit location, jet exit diameter, wing angle-of-attack, and the ratio of jet exit velocity to freestream velocity, λ . A comparison of the contours of constant interference surface pressure on the wing lower surface with those for an infinite flat plate reveals that they are much the same for $\lambda > 6$. The dissimilarity becomes greater as λ is decreased, primarily through the growth of an extensive region of positive interference surface pressure forward of the jet on the wing. Interference lift losses of approximately the same magnitude for all geometries were observed for $\lambda > 6$. However, a lift augmentation occurred for $\lambda < 6$ which was attenuated by increases in angle-of-attack, forward movement of the jet exit location, and decreases in jet exit size. The data indicate that the character of the interference flow is distinctly different for high and low values of the velocity ratio.

Nomenclature

c	= wing chord
C_p	= pressure coefficient, $(p - p_\infty)/q_\infty$
d_j	= jet exit diameter
L, D, PM	= total wing lift, drag, and pitching moment, respectively
p	= pressure
q	= dynamic pressure
T	= jet thrust
V	= velocity
x	= distance downstream from wing leading edge
α	= wing angle of attack
ΔC_L	= incremental lift coefficient
ΔC_p	= interference pressure coefficient
$\Delta D/T$	= interference drag coefficient
$\Delta L/T$	= interference lift coefficient
$\Delta M/Td_j$	= interference pitching moment coefficient
λ	= effective velocity ratio ($\lambda^2 = \rho_j V_j^2 / \rho_\infty V_\infty^2$)
ρ	= density

Subscripts

j	= jet exit plane
∞	= freestream conditions

Introduction

THERE is currently a strong interest in airplanes that utilize a direct lift jet or lift fan to provide a vertical take-off and landing capability. However, it is a well established fact that such airplanes generally suffer a lift loss and an adverse change in pitching moment during the transition from hovering to forward flight. These observed characteristics can be attributed to the aerodynamic interference created by the interaction of the lifting-jet efflux and the oncoming freestream and an accompanying effect on the adjacent lifting surface.

A large number of previous experimental investigations¹⁻⁸ have been concerned with determining the aerodynamic characteristics of complete VTOL aircraft configurations. Such investigations characteristically reveal the aforementioned lift loss and adverse pitching moment effects.

Received December 19, 1972; revision received May 7, 1973.

Index categories: Jets, Wakes, and Viscid-Inviscid Flow Interactions; VTOL Testing; Aircraft Aerodynamics (Including Component Aerodynamics).

*Graduate Research Assistant, presently a member of the Research Staff of The Rand Corporation, Santa Monica, Calif. Associate Member AIAA.

†Professor, School of Aerospace Engineering. Member AIAA.

However, the models tested were such as to make the extraction of fundamental results or the delineation of general trends very difficult.

The problem of a jet issuing from an infinite flat plate into a crossflow has also been widely studied and Refs. 9-12 are typical of these investigations. This configuration has merit since it is the simplest geometry that possesses the essential elements of the interference problem. Because of these works, coupled with a number of theoretical approaches such as Refs. 13 and 14, the problem of a jet effluxing from a flat plate can be considered reasonably well understood (with the exception of the wake region behind the jet).

The inherent motivation for the flat plate work is that such results are extensible to a jet issuing from a lifting surface. However, Williams and Wood¹⁵ have reported measurements obtained with a jet issuing from a finite rectangular wing which indicate possible shortcomings in this approach. In that investigation, extensive regions of positive interference surface pressure forward of the jet were noted on the wing which had no counterpart in the infinite flat plate case.

The link between experimental investigations dealing with jet efflux from complete VTOL aircraft configurations and from an infinite flat plate is the consideration of a jet issuing from a lifting surface. The majority of the previous efforts dealing with this simpler geometry have utilized a lifting fan imbedded in a finite wing. This type of configuration introduces the possibility of additional interference effects attributable to the fan inlet flow and the quality of the fan efflux.

Carter¹⁶ has recently attempted to overcome these difficulties by testing a finite rectangular wing with a jet supplied by an ejector system which was not an integral part of the wing model. This permitted the jet exit location to be easily varied but the closest the jet exit plane could be positioned was one-half a chord length beneath the wing. Interference force and moment measurements and a limited number of chordwise pressure measurements were made.

Finally, Wooler et al.¹⁷ have reported on the results of a jet issuing from a finite wing in which the jet air was supplied by a vertical pipe passing through the wing upper surface. This arrangement precluded direct measurements of the interference forces but chordwise pressure distributions were obtained at several span stations. Changes in the model angle of attack were not possible.

In the investigations of both Carter and Wooler, the arrangement of the jet air supply system may have caused significant mutual interference effects.

Experimental Configuration

An experimental configuration which overcomes many of the aforementioned objections is a wing model with an internal air supply and a good quality jet outflow. Such a model utilizing a modified NACA 0021 profile with a single circular jet exit on the lower surface was designed and built¹⁸ for testing in the Georgia Tech 9-ft low speed wind tunnel. The wing had a chord of 15 in. and spanned the tunnel thus permitting jet air to be supplied from both sides. As shown in Fig. 1, flat sidewalls were installed in the tunnel and the two-dimensional wing was mounted horizontally on the external wind tunnel balance pylons. This allowed a direct measurement of the total wing lift, drag, and pitching moment to be made with the existing balance system.

A plenum chamber was installed inside the wing at midspan as shown in Fig. 2. The chamber was designed to accommodate a variety of jet exit sizes and locations. For each configuration the jet nozzle consisted of a simple bellmouth with a straight extension to the wing surface. A calibration of the jets used in the test program, which was done by running them into still air, indicated satisfactorily flat exit plane velocity profiles and acceptable jet centerline decay characteristics in all cases. Air was supplied to this plenum chamber through flexible bellows connected to three hoses on each side (Fig. 2). Once outside the test section, a larger diameter flexible hose was used to bridge the tunnel balance system. These hoses were then connected to an external centrifugal compressor.

As can be seen in Fig. 2, the plenum chamber was isolated from the wing structure except at four flexures upon which strain gages were mounted. This arrangement allowed a direct measurement of the jet thrust to be made. (A dental dam seal was required at the jet nozzle/wing surface interface, Fig. 3.) The tunnel balance system was used to measure total wing forces and moments including the effects of the jet thrust. Hence, by considering the appropriate jet-off aerodynamic characteristics and the directly measured thrust, a simple calculation leads to the interference lift, drag, and pitching moment coefficients.

The major source of error in the interference force measurements came from the wind tunnel balance system. Balance lift readings were considered accurate to within ± 0.2 lb. This yields an estimated maximum possible error in $\Delta L/T$ of $\pm 4\%$ at $\lambda = 8$ and $\pm 20\%$ at $\lambda = 2$ (for $d_j/c =$

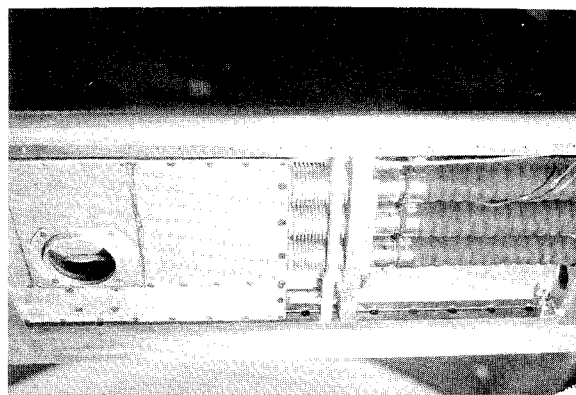


Fig. 2 The installation of the plenum chamber in the wing at mid-span. (Wing panel removed, view looking downstream.)

0.10). The accuracy deteriorates with decreasing λ because the reduction in the magnitude of the thrust results in the balance reading uncertainty becoming a greater percentage of the thrust value. For the larger jet ($d_j/c = 0.20$) the error in $\Delta L/T$ is within $\pm 5\%$ for all values of λ because of the correspondingly larger thrust levels. All data were repeatable within these maximum error bands. The interference drag and moment data are less accurate than the interference lift because of the small drag forces encountered and because of the pitching moment dependency on lift (transfer of reference axis to quarter chord) and drag (drag-pitch interaction from the model being mounted above the balance centerline). No wind tunnel wall corrections were made in the present work. Because of the large distance (5 ft) from the jet exit plane to the wind tunnel wall and the relatively small jet exit diameters used, wall effects caused by separation of the test section boundary layer due to jet impingement were not likely in these tests.

The wing was instrumented with 190 surface pressure taps. Approximately 60% of these taps were located in close proximity to the jet exit on the lower surface and another 30% were on the upper surface of the wing. The pressure lines were connected through scanivalves to four variable capacitance pressure transducers. Pressure measurements were made utilizing a Hewlett-Packard automated data acquisition system. The surface pressure coefficients are accurate to within $\pm 1\%$ and were repeatable to within $\pm 2\%$ in regions forward of and lateral to the jet and $\pm 4\%$ in the unsteady region aft of the jet.

Summary of Experimental Data

The configurations used in the experiments were: a single circular jet with a diameter/wing chord ratio of 0.10 at

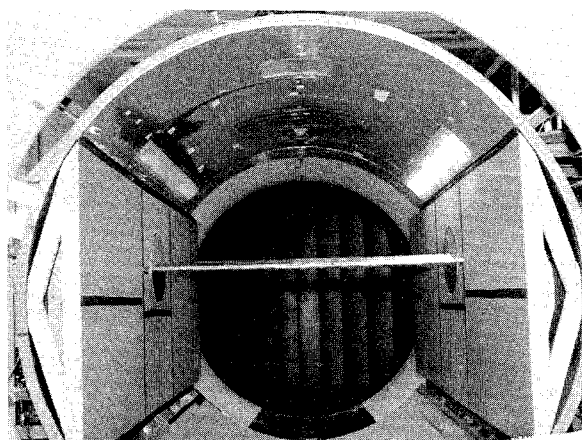


Fig. 1 The two-dimensional model as installed in the wind tunnel. (View looking upstream.)

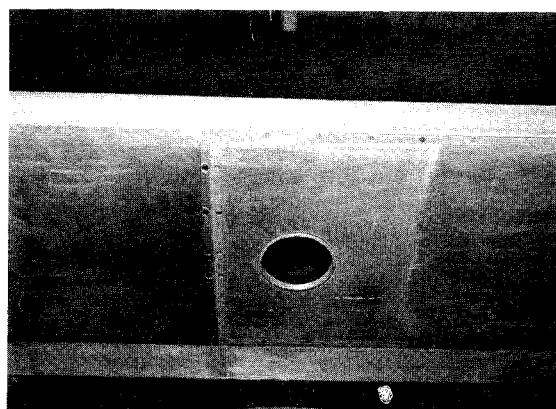


Fig. 3 Wing lower surface with 3-in. diam jet installed. (View looking downstream.)

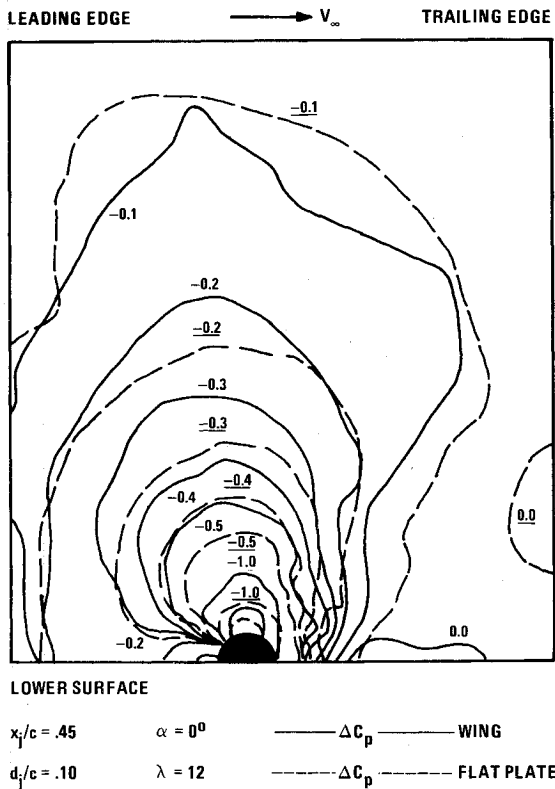


Fig. 4 Interference surface pressure contours for the wing and for a flat plate ($\lambda = 12$).

jet (centerline) exit locations of 25, 45 and 65% chord; and a single circular jet with a diameter/wing chord ratio of 0.20 at 45% chord. The testing was done in a range of wing Reynolds numbers from 2.5×10^5 to 1.2×10^6 .

Surface pressure measurements were made for each of these configurations at angles of attack of 0° , 6° , and 9° . Data were taken at values of effective velocity ratio, λ , of 2, 4, and 8 for all cases, and at $\lambda = 12$ for angle of attack 0° . The results are presented as interference pressure coefficients defined by

$$\Delta C_p = C_{p \text{ jet-on}} - C_{p \text{ jet-off}}$$

The contours of constant interference surface pressure were machine plotted for each case.

Interference lift, drag, and pitching moment measurements were made for all of the above conditions. In addition, these measurements were made for effective velocity ratios of 3, 6, 10, 12, and occasionally 2.5. These results are presented as

$$\frac{\Delta L}{T} = \frac{L_{\text{jet-on}} - L_{\text{jet-off}}}{T}$$

$$\frac{\Delta D}{T} = \frac{D_{\text{jet-on}} - D_{\text{jet-off}}}{T}$$

$$\frac{\Delta M}{Td_j} = \frac{PM_{\text{jet-on}} - PM_{\text{jet-off}}}{Td_j}$$

Note that, when the data are presented in this form, zero interference lift corresponds to $\Delta L/T = 1$. However, zero interference drag yields $\Delta D/T = 0$ and zero interference moment results in $\Delta M/Td_j = 0$.

Discussions of the Results

Comparison with Flat Plate Results

A comparison of the interference surface pressure contours on the wing lower surface with $d_j/c = 0.10$, $x_j/c =$

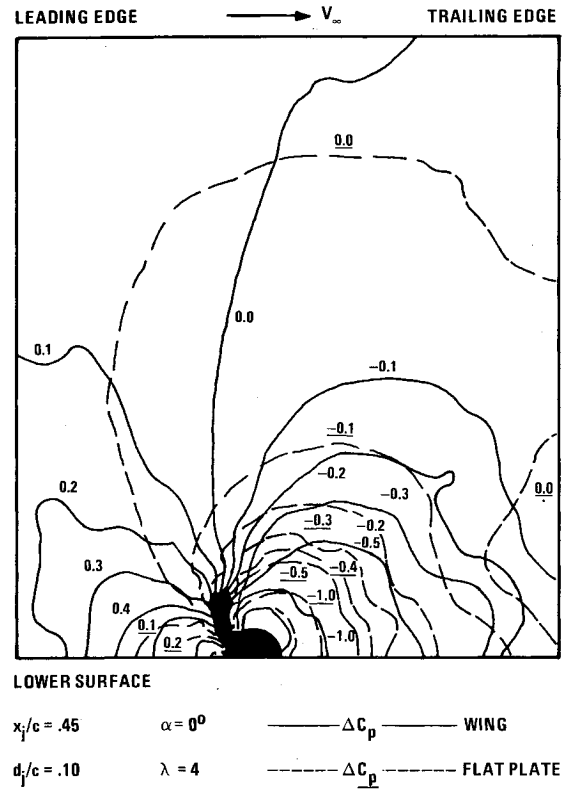


Fig. 5 Interference surface pressure contours for the wing and for a flat plate ($\lambda = 4$).

0.45, and $\alpha = 0^\circ$ and those on an infinite flat plate is made in Figs. 4 and 5. The flat plate interference pressures shown are those measured by Mosher.⁹ Figure 4 is the comparison at $\lambda = 12$ and, except in the immediate vicinity of the jet, the contours are very nearly identical. In Fig. 5 the comparison for $\lambda = 4$ shows a gross dissimilarity in the two cases. This difference is primarily concentrated in the region forward of the jet in which a significant spreading of positive interference pressure on the wing occurs that is rather localized on the flat plate to the immediate area in front of the jet. Also, the region of negative interference pressures aft of and lateral to the jet is somewhat more contained in the wing case.

The characteristics of the interference surface pressures on the wing were much the same for the other jet exit locations tested. In all cases, the effect of increasing angle of attack is primarily to decrease the extent of the region of positive interference pressure forward of the jet. For the larger jet ($d_j/c = 0.20$), this positive interference pressure region becomes much more extensive for all angles of attack. That is, the spreading is more than proportionate to the increase in jet diameter. For $d_j/c = 0.20$ and $\lambda \geq 8$, the similarity with the flat plate data is approximately the same as for the $d_j/c = 0.10$ case.

The existence and extent of a positive interference pressure region forward of the jet has also been reported by Williams and Wood.¹⁵ They commented on the results for a simple rectangular wing with a centrally located circular jet that at $\lambda = 4$ exhibited a region of strong positive interference pressure ahead of the jet that had no counterpart in the corresponding flat plate pressure distribution.

This region is essentially responsible for many of the gross aerodynamic characteristics of the wing to be noted later. A discussion of the cause of the forward positive pressure region is given in the section on physical interpretation.

In summary, a comparison of the interference surface pressures on the wing with the data for a flat plate indicates that for $\lambda \geq 8$ the jet issuing from the flat plate is a reasonable simulation of the lifting case. That is, the in-

terference surface pressure contours on the wing lower surface are approximately the same as those on the infinite flat plate for identical values of the effective velocity ratio. At values of $\lambda < 8$, the flow situation is vastly different. Subsequent discussion will indicate that the flow undergoes this character change for $4 < \lambda < 8$ and finally $\lambda \approx 6$ is used as the approximate boundary.

Parametric Comparison of the Aerodynamic Interference Characteristics

This comparison is made using the interference force and moment coefficients, which are expressed as a function of the effective velocity ratio, for the various geometric parameters used in the experiment. In this presentation the parameter $1/\lambda$ is used as the independent variable. This parameter, which ranges from zero in hovering flight to a practical maximum of about 0.5, is considered more natural in describing the interference aerodynamics of transitional flight. In each case, the reason for the observed behavior of the aerodynamic interference coefficients is primarily explained in terms of the corresponding interference pressure contours on the wing lower surface. The effect of jet operation on the wing upper surface was quite small for the $d_j/c = 0.10$ case. Characteristically, levels of interference surface pressure coefficients in the range $-0.10 < \Delta C_p < 0$ were induced by the jet on the upper surface and these levels did not vary appreciably with changes in effective velocity ratio, jet exit location, or angle of attack. Consequently, the changes in the aerodynamic interference coefficients can be attributed principally to the observed changes in the interference pressure distribution on the wing lower surface. However, somewhat more pronounced suction pressures were induced on the upper surface for $d_j/c = 0.20$ and the effect is noted later.

The variation of interference lift coefficient with effective velocity ratio is presented in Fig. 6 for the three an-

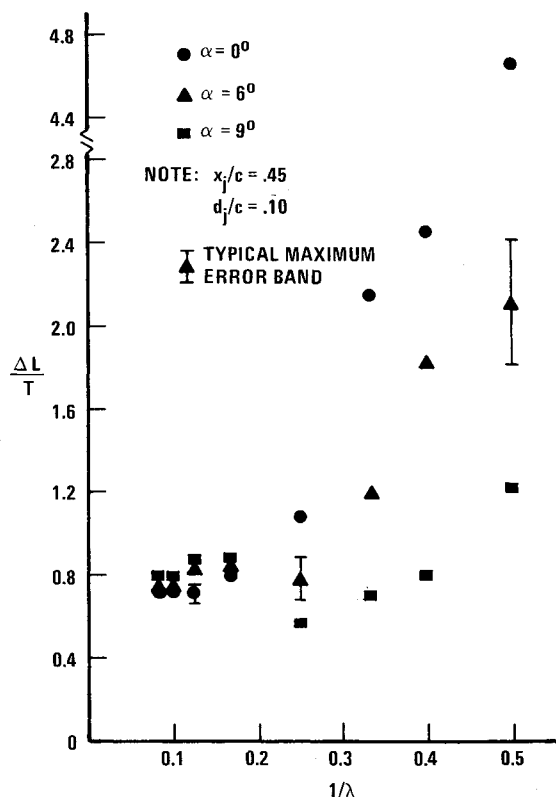


Fig. 6 Typical variation of interference lift coefficient with angle of attack.

gles of attack. In this figure, a significant lift augmentation occurs at $\alpha = 0^\circ$ for $\lambda < 6$ (i.e., $1/\lambda > 0.17$) and the augmentation effect decreases with increasing angle-of-attack. The reader is reminded that zero interference lift corresponds to $\Delta L/T = 1$ (i.e., for a lift loss, $\Delta L/T < 1$ and for a lift augmentation, $\Delta L/T > 1$). Note that for all angles of attack a reversal of the observed trends occurs for $\lambda \approx 6$. A study of the corresponding interference surface pressure distribution indicates that the region of positive interference pressure forward of the jet is mainly responsible for the lift augmentation. (Reiterating, only minor changes characterized by small induced negative interference pressures that did not vary with λ were observed on the upper surface.) The extent of the positive interference pressure region decreases correspondingly with increasing angle of attack. Note also that the adverse interference effect for $\lambda \geq 6$ is alleviated somewhat by increasing incidence. For this alleviation, which is a small effect, a very slight increase in the extent of the positive interference pressure region and a correspondingly small decrease in the region of negative interference pressures aft of and lateral to the jet is noticeable.

Figure 7 shows typical trends for the interference drag coefficient and the interference pitching moment coefficient. The significant drag rise and increase in adverse (i.e., nose up) pitching moment is characteristic of values of λ for which the lift augmentation was observed. These trends are consistent with the noted behavior of the interference surface pressures.

The effect of jet exit location on the interference lift coefficient is presented in Fig. 8. Not surprisingly, the lift augmentation increases as the jet exit location is moved aft. This is attributed to the increased area available for the positive interference pressures forward of the jet. (However, on the basis of flat plate data one might have assigned this effect to a decrease in the area available to the negative interference pressures aft of the jet.) Again, for the cases of alleviated detrimental effects for $\lambda \geq 6$ (these occur for $x_j/c = 0.25$ and $x_j/c = 0.65$) a slight increase in the extent of the positive interference pressure region and a minor contraction of the negative interference pressure region is ascertainable.

Carter¹⁶ has observed a similar behavior of the interference lift coefficient with jet exit location. He reported interference lift losses that were reversed at $\lambda \approx 6$ and also

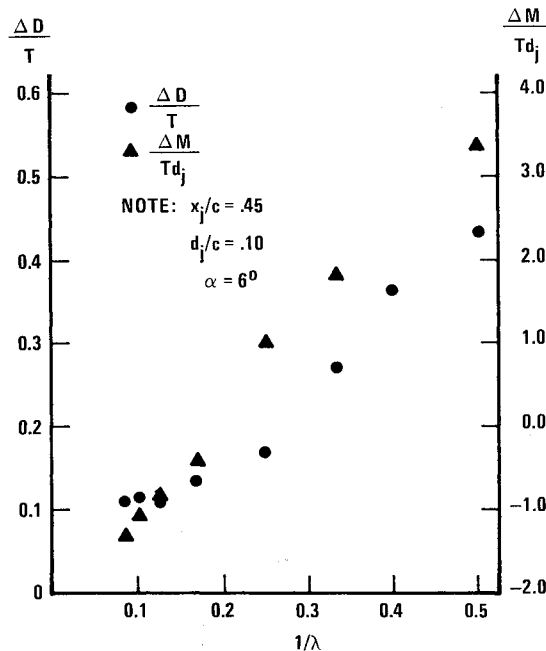


Fig. 7 Typical behavior of the interference drag coefficient and the interference pitching moment coefficient.

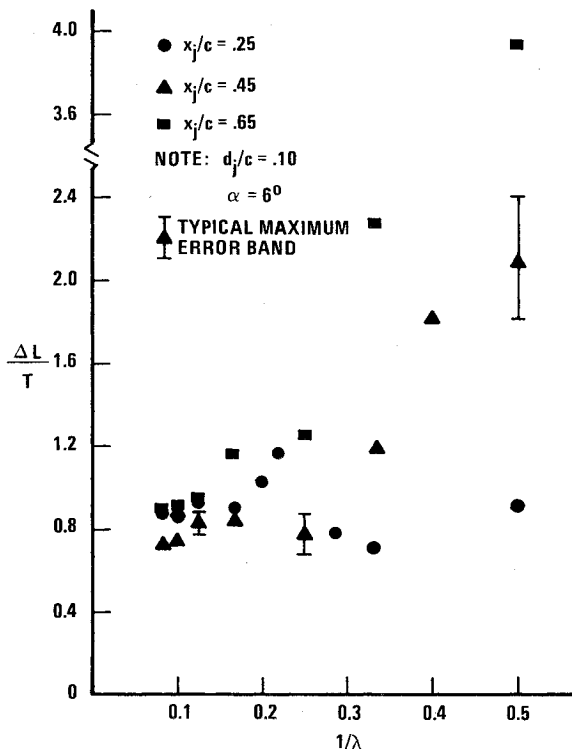


Fig. 8 Typical variation of interference lift coefficient with jet exit location.

an increasing lift augmentation as the jet location was moved aft. However, the lift augmentation noted in that work was not nearly of the magnitude observed here. This is probably a result of Carter's experimental configuration in which the nearest the jet exit plane could be positioned was 0.64 wing chords beneath the wing chordal plane. In Carter's work, chordwise pressure distributions at the span station which contained the jet exit centerline

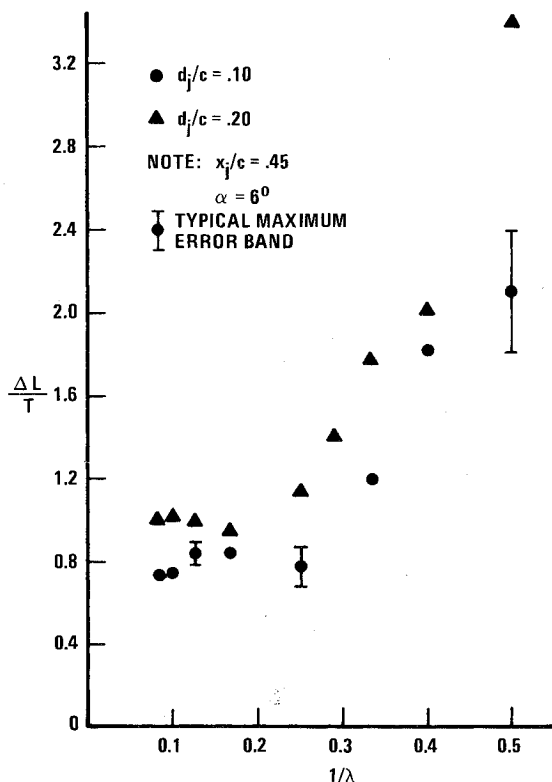


Fig. 9 Typical variation of interference lift coefficient with jet exit size.

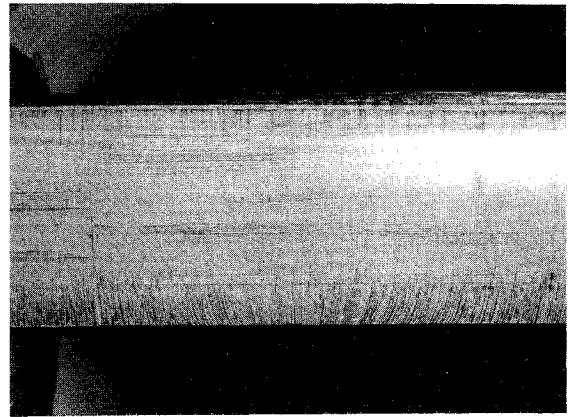


Fig. 10 Oil flow for the 3-in.-diam jet ($d_j/c = 0.20$) at $\lambda = 2$ and $\alpha = 0^\circ$ (Upper surface).

showed only small positive interference pressures forward of the jet exit at $\lambda = 4$. The magnitude of those interference pressure coefficients for $x_j/c = 0.75$ was about half that observed in the present investigation at $x_j/c = 0.65$. Conversely, Carter reported much larger positive interference pressure coefficients forward of the jet for $x_j/c = 0.75$ at $\lambda = 10$. These results suggest that the interference flow characteristics are different when the jet exit plane does not coincide with the wing surface.

Lastly, Fig. 9 presents the effect of jet exit diameter on interference lift coefficient. The larger jet ($d_j/c = 0.20$) provides a comparatively favorable effect throughout the range of λ . This is again attributed to the region of positive interference pressure forward of the jet for $\lambda < 6$. In the case of $d_j/c = 0.20$, this region is much more extensive than a direct scaling of the exit diameters would predict. However, an increase in the suction pressures induced by the jet on the wing upper surface is primarily responsible for the favorable effect in the $\lambda > 6$ range.

An examination of Figs. 6, 8, and 9 shows that in all cases a reversal of the trends discussed occurs at $\lambda \approx 6$. This fact constitutes the point made earlier with regard to the pressure data that the character of the interference flow undergoes a change at about this effective velocity ratio.

Physical Interpretation

The agreement of the wing interference characteristics with those of the flat plate for $\lambda > 6$ is quite pronounced. The similarity is evident for both the interference surface pressure contours and the corresponding detrimental interference lift which would be predicted by an integration of the surface pressure on the flat plate. Thus, for these higher effective velocity ratios, the jet interference effects are nearly independent of the geometric characteristics of the adjacent surface. The jet does induce small suction pressures on the upper surface of the wing that are not sensitive to changes in wing angle of attack or jet exit location. These suction pressures are a result of the downwash field that is created by jet operation.

In this range of higher effective velocity ratios, the observed small increase in the region of positive interference pressure forward of the jet and the moderate contraction of the negative interference pressure region lateral to the jet with increasing angle of attack can be explained by appeal to an apparent λ change. That is, the jet exit dynamic pressure in the experiment was set by assuming the jet exit static pressure always to be the freestream static value. Thus, regardless of the wing angle-of-attack or the jet exit location, the same ratio of plenum chamber stag-

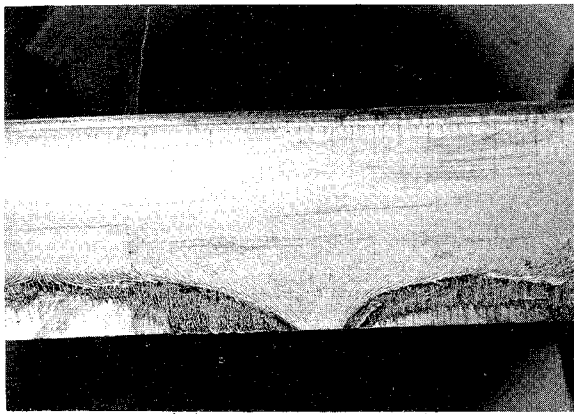


Figure 11. Oil flow for the 3-in.-diam jet ($d_j/c = 0.20$) at $\lambda = 2$ and $\alpha = 9^\circ$ (Upper surface).

nation pressure to freestream static pressure was used to set a particular value of λ . However, as the angle of attack is increased the actual local static pressure at the jet exit on the wing lower surface is also increased and hence a smaller jet exit Mach number and a smaller jet exit dynamic pressure results. The net effect is a decrease in the effective velocity ratio λ . This small decrease in the apparent value of λ is thought to account for the observed pressure trends since these trends agree with those noted for changes in λ as reported in Ref. 9. This same effect is present when the jet exit location is changed. There is an increase in the local static pressure at $x_j/c = 0.25$ and 0.65 with respect to the $x_j/c = 0.45$ value. Correspondingly, there are small increases in the areas of positive interference pressure forward of the jet and contractions of the negative interference pressure regions lateral to the jet for these two chordwise jet locations when compared with the jet at $x_j/c = 0.45$.

For the lower effective velocity ratio range ($\lambda < 6$), the entire character of the interference flow is decidedly different. The lifting jet-crossflow interaction begins to exhibit characteristics usually associated with a jet flap, even though the configuration tested has an extensive and complex three-dimensional wake which the classical jet flap does not. A jet-flap provides a lift augmentation by inducing an increased effective angle of attack through downwash while simultaneously allowing a nonzero pressure differential at the wing trailing edge.¹⁹ This latter effect is possible because the deflected jet-flap can support a pressure differential (the so-called supercirculation effect). A direct result is an alleviation of the adverse pressure gradient on the wing upper surface thus delaying any boundary-layer separation.

The experimental evidence that a jet-flap effect is occurring is reinforced by the flow visualizations shown in Figs. 10-12. In the oil flow figures, the wing has been rotated 90° with the leading edge up before being photographed. In Fig. 10, note that the upper surface streamlines in the vicinity of the wing centerline (at the center of the figure) are showing an inward turning due to the influence of the jet operation. The effect at $\alpha = 9^\circ$ is more dramatic as shown in Fig. 11 where the local prevention of boundary-layer separation is obvious. More surprising, however, is the standing vortex aft of the jet exit shown in Fig. 12. This vortex was not observed for the same test conditions as Fig. 12 but with $\alpha = 0^\circ$. (The presence of this standing vortex was not discovered until the very end of the experimental program because it was felt that no oil flow studies should be made until all the surface pressure data had been gathered since the possibility of having the oil mixture migrate into the surface pressure lines existed. Other demands on wind tunnel time prohibited further investigation.) Finally, a close examination of the

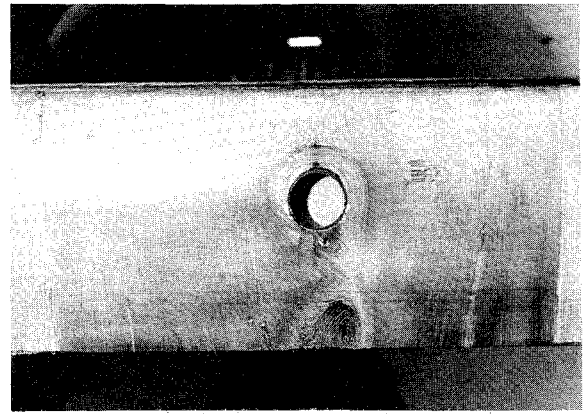


Fig. 12 Oil flow for the 3-in.-diam jet ($d_j/c = 0.20$) at $\lambda = 2$ and $\alpha = 9^\circ$ (Lower surface).

chordwise pressure distributions for the $\lambda < 6$ range provides evidence that a nonzero pressure differential at the trailing edge exists locally in the region aft of the jet.

The region of positive interference pressures forward of the jet is thought to be a direct result of the induced downwash which is characteristic of jet-flap installations. The magnitude of these pressure changes are much in line with those reported by Dimmock²⁰ in which an elliptical profile with a pure jet-flap was investigated. A comparison of his results with a chordwise pressure distribution of the present investigation for similar effective velocity ratios is presented in Fig. 13 (the parameter of importance in the jet-flap case is the jet momentum coefficient which in the cited example corresponded to a $\lambda \approx 2$). Note that the positive interference pressures forward of the jet (i.e. lower surface) are nearly identical in both cases up to $x/c \approx 0.35$. The interference pressures become more positive for the present study as the jet exit location ($x_j/c = 0.65$)

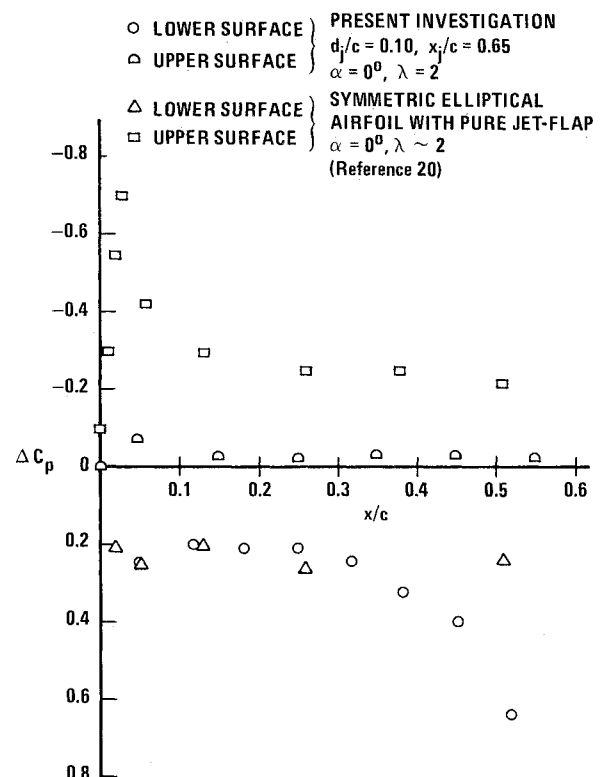


Fig. 13 Comparison of the chordwise interference pressure distribution of the present model at the wing centerline with that of a two-dimensional symmetric elliptical airfoil equipped with a pure-jet-flap (Ref. 20).

is approached but this deviation should be expected since Dimmock's jet-flap was located at the trailing edge. This comparison demonstrates that the increase in the extent of the induced positive pressures may be attributable to the jet-induced downwash. Recalling that moderate positive interference pressures forward of the jet already exist for the flat plate case at these effective velocity ratios, it is reasoned that a moderate induced angle of attack would produce the positive interference pressures observed on the wing.

To readers familiar with the behavior of jet-flaps, the lift augmentation shown in Figs. 6, 8, and 9 may appear at first glance to be the opposite of the behavior of a jet-flap. Jet-flap results are normally described in terms of an incremental lift coefficient expressed as $\Delta C_L = (C_L)_{\text{jet-on}} - (C_L)_{\text{jet-off}}$. In the jet-flap case, ΔC_L decreases with a decrease in the jet momentum coefficient. If the present results were presented in incremental lift coefficient form, then $\Delta C_L \approx (\Delta L/T)(T/q_\infty) \approx (\Delta L/T)(\lambda^2)$ so that (assuming the effect of compressibility is small) ΔC_L decreases with decreasing λ (i.e. decreasing jet exit velocity) because λ^2 decreases faster than $\Delta L/T$ increases.

Collectively, these facts indicate that the behavior of this lifting jet is similar to a jet-flap installation. However, it must be noted that the fundamental mechanisms responsible for this behavior may be quite different in the two cases. That is, the principal mechanism of the jet-flap is the solid blockage effect that the jet momentum efflux provides. In the case of the lifting jet, the entrainment effect may be more significant.

Characteristically, however, a jet-flap induces large suction pressures (particularly near the leading edge) on the wing upper surface. Only small induced suction pressures were noted in the present investigation for $d_j/c = 0.10$. The magnitude of the difference in the upper surface interference pressure coefficients for the two cases can be seen in Fig. 13. The absence of large upper surface suction pressures in this investigation can be attributed to the rather poor jet-flap installation the current configuration affords. That is, the lifting jet efflux is much too far forward to be a truly effective jet-flap. However, for the larger jet ($d_j/c = 0.20$), the interference pressure coefficients on the upper surface displayed the suction effect to a greater degree. The magnitude of these pressures was again much less than an efficient jet-flap would produce.

Finally, it must be remarked in light of the insensitivity to changes in flow conditions of the small induced suction pressures on the upper surface that the positive interference pressure region on the lower surface is the dominant characteristic of the flow which is responsible for the lift augmentation. Further evidence of this is contained in Figs. 10 and 11. In Fig. 11 at $\alpha = 9^\circ$ the local improvement in the flow over the wing upper surface is considerable when compared with Fig. 10 but the lift augmentation of the larger jet was found to be less in the $\alpha = 9^\circ$ case, thus indicating that the decrease in the positive interference pressure region overshadows the upper surface effect.

Conclusions

An analysis of the data collected in this experiment has led to the following conclusions.

1) A comparison of the interference surface pressure distributions on the wing with those on the flat plate indicates that flat plate results are not wholly applicable when the jet efflux is from a lifting surface. The discrepancy between these interference pressure contours is quite small for values of the effective velocity ratio larger than six. However, for effective velocity ratios less than six in the lifting case a large increase occurs in the extent of the

region of positive interference pressure forward of the jet which has no counterpart on the infinite flat plate.

2) Interference lift losses were observed for all jet exit geometries when the effective velocity ratio was greater than six. A lift augmentation in which the favorable interference lift was significantly larger than the installed thrust occurred for effective velocity ratios less than six and is attributed to extensive increases in the region of positive interference surface pressure forward of the jet. This lift augmentation was accompanied by a large interference drag rise and an adverse (became more positive) increase in the interference pitching moment.

3) The effect of jet operation on the wing upper surface for $d_j/c = 0.10$ was characterized by small induced suction pressures, the level of which was insensitive to changes in effective velocity ratio, angle of attack, and jet location. Consequently, changes in the lower surface interference pressure distribution were primarily responsible for the aerodynamic interference behavior observed. Somewhat larger suction pressures were induced on the upper surface for $d_j/c = 0.20$ which were sufficient to alleviate the lift losses observed for $\lambda > 6$ and $d_j/c = 0.10$.

4) Increases in wing angle of attack resulted in a decrease in the magnitude of the lift augmentation for $\lambda < 6$ because of a corresponding shrinkage in the extent of the positive interference pressure region forward of the jet.

5) The lift augmentation is magnified as the jet exit location is moved aft since an increase is provided in the area available to the positive interference surface pressure region forward of the jet.

6) As the jet diameter/wing chord ratio is increased, the lift augmentation becomes moderately larger due to a wider spreading of the forward region of positive interference pressure for the larger jet.

7) Changes in wing angle of attack or jet exit location have only a moderate effect on the magnitude of the detrimental interference lift losses which occur for values of the effective velocity ratio in excess of six.

8) As the effective velocity ratio is decreased from six, the interaction of the lifting jet efflux and the wing begins to exhibit behavior similar to a jet-flap. The "jet-flap effect" is thought to be responsible for the behavior of the positive interference pressure region forward of the jet which is the dominating factor in the lift augmentation.

References

- ¹Vogler, R. D., "Interference Effects of Single and Multiple Round or Slotted Jets on a VTOL in Transition," TN D-2380, Aug. 1964, NASA.
- ²Spreeman, K. P., "Induced Interference Effects on Jet and Buried-Fan VTOL Configurations in Transition," TN D-731, March 1961, NASA.
- ³Otis, J. H., "Induced Interference Effects on a Four-Jet VTOL Configuration with Various Wing Planforms in the Transitional Speed Range," TN D-1400, Sept. 1962, NASA.
- ⁴Margason, R. J. and Gentry, G. L., "Aerodynamic Characteristics of a Five-Jet VTOL Configuration in the Transition Speed Range," TN D-4812, Oct. 1968, NASA.
- ⁵Margason, R. J., "Review of Propulsion Induced Effects on Aerodynamics of Jet/STOL Aircraft," TN D-5617, Feb. 1970, NASA.
- ⁶Kirk, J. V., Hodder, B. K., and Hall, L. P., "Large Scale Wind Tunnel Tests of a V/STOL Transport Model with Wing-Mounted Lift Fans and Fuselage Mounted Lift-Cruise Engines for Propulsion," TN D-4233, 1967, NASA.
- ⁷Hickey, D. and Hall, L., "Aerodynamic Characteristics of a Large-Scale Model with Two High Disc-Loading Fans Mounted in the Wing," TN D-1650, Feb. 1963, NASA.
- ⁸Maki, R. L. and Hickey, D. H., "Aerodynamics of a Fan-in-Fuselage Model," TN D-789, 1961, NASA.
- ⁹Mosher, D. K., "An Experimental Investigation of a Turbu-

lent Jet in a Crossflow," Ph.D. Thesis, Dec. 1970, Georgia Inst. of Technology, Atlanta, Ga.

¹⁰Keffer, J. G. and Baines, W. D., "The Round Turbulent Jet in a Cross Wind," *Journal of Fluid Mechanics*, Vol. 15 Pt. 4, 1963, pp. 481-496.

¹¹Jordinson, R., "Flow in a Jet Directed Normal to the Wind," R & M 3074, Oct. 1956, British Aeronautical Research Council, London, England.

¹²Bradbury, L. J. S. and Wood, M. N., "The Static Pressure Distribution Around a Circular Jet Exhausting Normally from a Plane Wall into an Airstream," TN 2978, Aug. 1964, British Royal Aircraft Establishment, Farnborough, England.

¹³Wooler, P. T., "On the Flow Past a Circular Jet Exhausting at Right Angles from a Flat Plate or a Wing," *Journal of the Royal Aeronautical Society*, Vol. 71, March 1967, pp. 216-218.

¹⁴Margason, R. J., *Analysis of a Jet in a Subsonic Crosswind*, NASA SP-218, Sept. 1969.

¹⁵Williams, J. and Wood, M. W., "Aerodynamic Interference Effects with Jet-Lift V/STOL Aircraft under Static and Forward-

Speed Conditions," *Zeitschrift fur Flugwissenschaften*, Vol. 15, No. 7, July 1967, pp. 237-256.

¹⁶Carter, A., "Effects of Jet-Exhaust Location on the Longitudinal Aerodynamic Characteristics of a Jet V/STOL Model," TN D-5333, July 1969, NASA.

¹⁷Wooler, P. T., Burghart, G. H. and Gallagher, J. T., "The Pressure Distribution on a Rectangular Wing with a Jet Exhausting Normally into an Airstream," *Journal of Aircraft*, Vol. 4, No. 6, Nov.-Dec. 1967, pp. 537-543.

¹⁸Mikolowsky, W. T., "An Experimental Investigation of a Jet Issuing from a Wing in Crossflow," Ph.D. thesis, May 1972, Georgia Inst. of Technology, Atlanta, Ga.

¹⁹Williams, J., Butler, S. F. J., and Wood, M. N., "The Aerodynamics of Jet-Flaps," R & M 3304, Jan. 1961, British Aeronautical Research Council, London, England.

²⁰Dimmock, N. A., "An Experimental Introduction to the Jet-Flap," C. P. 344, 1957, British Aeronautical Research Council, London, England.